

Full length article

Assessing outdoor air quality and public health impact attributable to residential black carbon emissions in rural China



Yefu Gu^a, Weishi Zhang^{b,c,*}, Yuanjian Yang^{a,d}, Can Wang^c, David G. Streets^f, Steve Hung Lam Yim^{a,e,g,*}

^a Department of Geography and Resource Management, The Chinese University of Hong Kong, Hong Kong, China

^b School of Geographic and Environmental Sciences, Tianjin Normal University, Tianjin 300387, China

^c State Key Joint Laboratory of Environment Simulation and Pollution Control (SKLESPC), and School of Environment, Tsinghua University, Beijing 100084, China

^d School of Atmospheric Physics, Nanjing University of Information Science and Technology, Nanjing, China

^e The Institute of Environment, Energy and Sustainability, The Chinese University of Hong Kong, Shatin, N.T., Hong Kong, China

^f Energy Systems Division, Argonne National Laboratory, Argonne, Illinois 60439, United States

^g Stanley Ho Big Data Decision Analytics Research Centre, The Chinese University of Hong Kong, Shatin, N.T., Hong Kong, China

ARTICLE INFO

ABSTRACT

Keywords:

Residential consumption
Black carbon
Premature mortality
Concentration response
CMAQ
Regional transportation

Black carbon (BC) is a significant component of particulate matter (PM) that relates to air pollution, climate forcing, and further implications for public health. BC is predominantly released from the combustion of solid fuels. Combustion of low-quality fuels in rural China may induce severe respiratory and cardiopulmonary health outcomes for residents, which have however been inadequately assessed. One major reason for the limited understanding is the lack of a high-resolution inventory. An improved method of estimating the BC-associated public health burden is needed. This work quantified premature mortalities due to residential BC emissions in rural China. Domestic BC emissions at 1 × 1 km resolution were compiled based on previous field investigation, which were further configured for air quality simulation. A chemistry transport model, WRF-CMAQ v5.2, was employed for simulating BC concentrations. The consequent premature mortalities were quantified by a BC-specific concentration-response function (CRF) derived from an epidemiological study. Results show that residential combustion of solid fuel in rural China emitted 648.0 Gg (95%CI: 361.0–965.9) BC in 2014, after dispersion, accounting for 51.8% of annual mean ground-level BC concentration in China. Such impact was most severe in North and Northeast China, and the Sichuan Basin. The further investigation estimated 171,000 (95%CI: 69,000–387,000) premature mortalities that were attributable to exposure to rural residential BC. These findings reveal the major contribution of rural residential BC emissions to air pollution formation and public health impacts. Our findings are anticipated to provide useful information for enacting the next-stage environmental strategy for the residential sector in China.

1. Introduction

Anthropogenic activities, including the direct combustion of solid fuels (straw, wood, agricultural waste, and coal), have been reported to be the major source of indoor air pollution (WHO, 2007). In rural areas, the direct combustion of solid fuels by households is a major source of combustion-related black carbon (BC), especially in developing countries (Streets and Aunan, 2005). China is the largest contributor to global BC emissions (Bond et al., 2013), and 50–70% of BC emissions in China are from residential solid fuel consumption (Bond et al., 2013; Streets et al., 2001; Streets and Aunan, 2005). In recent decades, air pollution levels have been significantly reduced as a result of a series of

emission control policies, mostly focusing on the industry, energy, and transportation sectors (Jin et al., 2016; Sun et al., 2018; Yuan et al., 2018).

Most rural households spend a large portion of time indoors, in which children and women are particularly vulnerable because of poor ventilation in most rural Chinese kitchens and bedrooms (Weishi Zhang et al., 2018a). Increasing scientific research reported that PM exposure is closely related to a wide array of adverse health effects (Lim et al., 2012). It has been reported that residential PM is responsible for approximately 5.1% of the global total mortalities (Cohen et al., 2017). BC as a significant component of PM was found to be associated with multiple adverse health effects (Highwood and Kinnersley, 2006;

* Corresponding author.

E-mail addresses: zhangweishi@link.cuhk.edu.hk (W. Zhang), steveyim@cuhk.edu.hk (S.H.L. Yim).

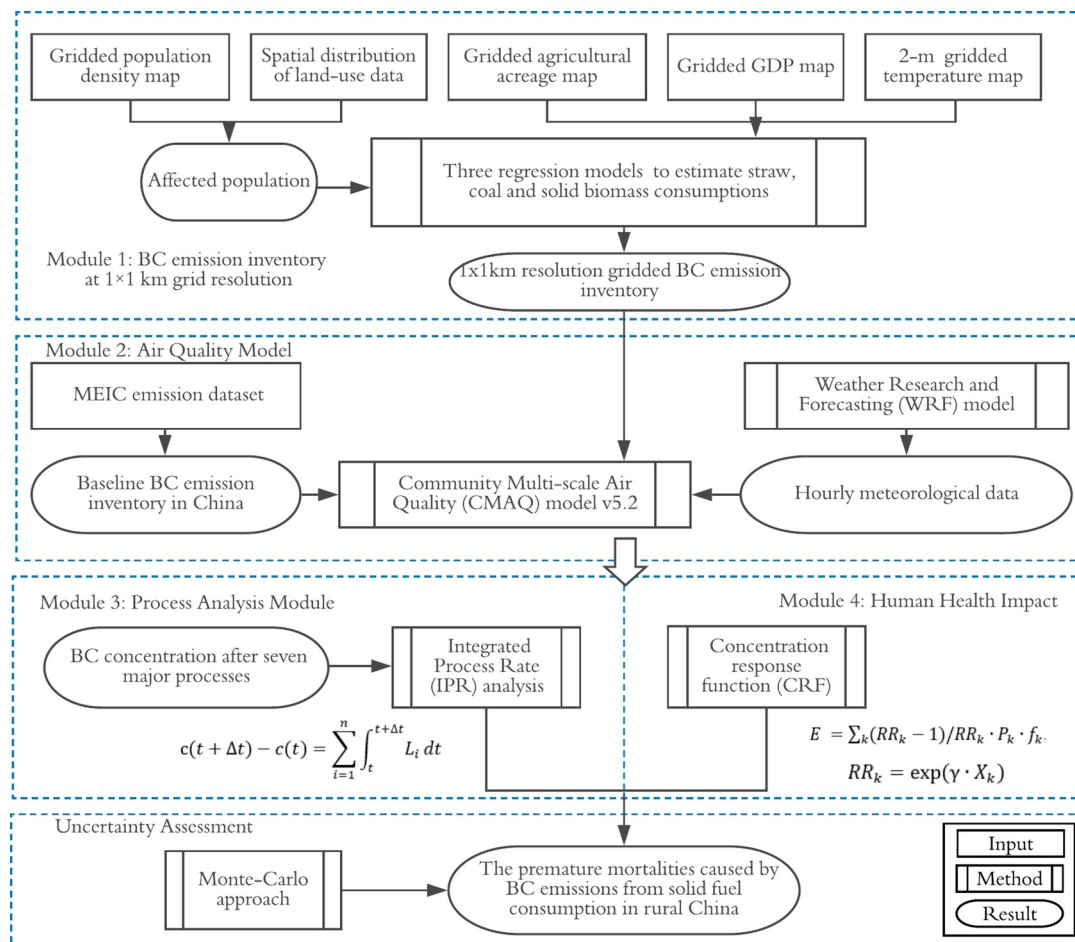


Fig. 1. Schematic diagram of the components of this study

Suglia et al., 2007; WHO, 2012), in particular for the premature mortality under long-term and short-term exposures (Anderson et al., 2012). Recent research shows that, per mass unit, BC particles are more toxic to public health than total PM (Bell et al., 2009; Lipfert et al., 2006; Peng et al., 2009).

Given the increasing emission contributions and higher health risk, the assessments of the impacts of residential BC emissions in rural China are still lacking. One reason for the limited understanding of the impacts of rural residential BC emission is lacking accurate estimations of BC emissions in China by energy consumption types. In previous research, BC emissions in China were extracted from global inventories (Penner et al., 1993; Streets et al., 2001). More recently, BC emissions were calculated based on emission factors and energy consumption (Wang et al., 2012), and energy consumptions were estimated by a top-down method that apportioned local consumption from national, annual statistics, within which many homogeneous assumptions induced additional uncertainties. As a result, BC emissions from residential combustion of solid fuels were estimated to have a large variability, ranging between 444 and 1117 gigagram (Gg) in the period 1996–2009 (Chen et al., 2009; Streets et al., 2001; Wang et al., 2012).

Another contributing factor to the inconsistency of previous research is the lack of a reliable method of quantifying the health impact specific to BC exposure. Previous research assumed an equal risk associated with a concentration increase when calculating premature mortalities under the exposure of different PM components (Anenberg et al., 2011; Saikawa et al., 2009). The concentration-risk (CR) relationship for BC has been poorly addressed in previous literature. Janssen et al. (2011) recently put forward a risk coefficient range

for the health effects of BC through a meta-analysis based on previous BC cohorts. These coefficients were used in assessing morbidity and mortality due to BC exposure in the US in 2010 (Li et al., 2016). The authors found that premature deaths are approximately ten times greater when using the BC-specific risk coefficient compared to the results using a PM_{2.5} coefficient (Krewski et al., 2009). It is, therefore, necessary to assess the health impact of rural residential BC emissions in China by developing a detailed BC emission inventory and a BC-specific concentration-response function to reflect the higher toxicity of BC.

Incomplete representation of BC toxicity, together with rough emissions estimation method, might introduce significant bias and uncertainties in quantifying the health burden of residential emissions in previous studies. This work systematically investigated the premature mortalities attributed to BC emissions from residential sources in rural China. We applied a bottom-up approach to estimate BC emissions from rural residential sources. The emissions were then compiled and input to the state-of-the-science chemistry transport model, CMAQ v5.2, to simulate the concentration impact. The health outcomes were calculated based on the concentration-response function specific to BC exposure. The rest of the work is structured as follows: In Section 2, the material and methods adopted in this work are introduced; in Section 3, the BC emission inventory at 1 × 1 km resolution, dispersion impacts and the corresponding formation mechanism, and the resultant health burden are assessed. Based on the key findings, Section 4 discusses the significances of this research in the context of filling the research gap and policy suggestions. Peer evaluations and limitations were also discussed for future efforts.

2. Materials and methods

We adopted an integrated method to estimate the health burden related to BC exposure due to solid fuel combustion in rural China. In [Section 2.1](#), we estimated the BC emissions related to solid fuel combustion with a resolution of 1×1 km over rural China. [Sections 2.2](#) and [2.3](#) describe the chemistry transport model and the process analysis tools for converting BC emissions to ambient concentration levels. In [Section 2.4](#), we present the concentration-response function (CRF) used to estimate the number of premature mortalities and the corresponding coefficients specific for quantifying BC exposure. The uncertainties involved in estimating emissions, concentrations, and premature mortalities are described in [Section 2.5](#). A schematic diagram for the connections between the various components of this study is provided in [Fig. 1](#).

2.1. BC emissions in rural China at 1×1 km resolution

We calculated the BC emissions released from coal and solid biomass combustion at 1×1 km grid resolution based on the bottom-up method provided by [Zhang et al., 2018b](#), which enhanced the accuracy of BC emissions generated from anthropogenic activities in rural China. The uncertainties of the inventory were quantified by adopting a Monte Carlo simulation (10,000 runs). Emissions of BC from solid fuel consumption at 1×1 km resolution, denoted by EM_i , were calculated as:

$$EM = \sum_{n,f,i} HN_i \cdot SH_{n,i} \cdot EF_{n,f} \cdot FU_{n,f,i} \quad (1)$$

where n denotes the stove type is either traditional stove or the improved type; f is the solid fuel types, which are coal, straw and wood; i refers to 1×1 km grid. HN refers to rural household numbers exposed to BC pollution, which was estimated through the affected population (Pop) divided by the average number of people per household. The rural household scale for each province in 2014 was obtained from the China Statistical Yearbook ([National Bureau of Statistics of China, 2015](#)). The Pop indicates the number of people exposed to BC pollution due to solid biomass combustion in rural areas. Population information was calculated based on the 1×1 km spatial distribution of population density in 2010 and 2015, and then linearly interpolated to the population in 2014. Rural area coverage in China was resolved from land-use data and light data from DMSP/OLS ([Imhoff et al., 1997](#)). Detailed information on the division between urban and rural areas are provided in the Supporting Information (SI), [Section 1](#). Population density in 2010 and 2015, land use data, and nighttime light data were obtained from the Resource and Environment Data Cloud Platform and the Chinese Academy of Sciences (CAS-REDCP) ([Liu et al., 2014](#)). BC emission factors (EF), were obtained from multiple studies for different fuel types and stove types as discussed in our previous study ([Zhang et al., 2018b](#)). The energy consumption of straw (FU_{STRAW}), total biomass (FU_{TB}), coal (FU_{COAL}) and wood (FU_{WOOD}) per household was estimated by three separate functions:

$$FU_{STRAW} = \alpha_f \cdot (56.0 + 0.5 \cdot AC - 0.003 \cdot IC + RI + \varepsilon) \quad (2)$$

where $RI_{Central\ South} = -76.6$; $RI_{Northeast} = 938.4$

$$FU_{TB} = \alpha_f \cdot (400.0 + 0.6 \cdot AC - 0.005 \cdot IC + RI + \varepsilon) \quad (3)$$

where $RI_{North} = -326.0$, $RI_{Northeast} = 346.6$, $RI_{Southwest} = 181.5$, $RI_{Northwest} = -198.8$.

$$FU_{COAL} = \alpha_f \cdot (805.4 - 51.5 \cdot T + 0.05 \cdot IC + RI + \varepsilon) \quad (4)$$

where $RI_{North} = 682.9$; $RI_{Northeast} = -1075.2$; $RI_{East} = -555.4$; $RI_{Southwest} = 502.4$

$$FU_{WOOD} = FU_{TB} - FU_{STRAW} \quad (5)$$

where the values of regional fixed effects (RI) and model correction factors (α_f) were derived from previous regressions of field survey

samples ([Zhang et al., 2018b](#)). AC and IC respectively denote cultivated area per capita (m^2) and income per capita (CNY) in each grid cell. Cultivated land was determined from land use information. Gridded income was obtained from IGSNRR. Annual and monthly 2-m temperature (T , °C) was interpolated from the ground-level temperature measurement based on smoothing splines. The gridded technology shares of improved combustion stoves (SH_{Imp}) is a function of the average household income (HI , CNY) and T , which could be resolved as:

$$SH_{Imp} = \frac{\exp(-9.394 + 1.657 \cdot \log(HI) - 0.178 \cdot T)}{1 + \exp(-9.394 + 1.657 \cdot \log(HI) - 0.178 \cdot T)} \quad (6)$$

where HI is the household income, which was estimated as IC multiplied by rural household scale. The share of traditional combustion stoves (SH_{trad}) is the technique portion other than SH_{Imp} .

To compile the model-ready emission inventory, hourly BC emissions from coal burning were allocated from annual BC emissions at the corresponding location and a conversion factor inversely related to the ambient outdoor temperature, since the energy consumption of coal is negatively associated with temperature, as described in [Eq. \(4\)](#). For straw and wood combustion, monthly and hourly profiles were applied to convert the annual BC emission inventory to hourly emissions ([Olivier et al., 2003](#)). Specifically, monthly emission profiles were derived from the study by Zhou et al. describes the monthly variation of different biomass emission sources in different regions in China ([Zhou et al., 2017](#)). Hourly emission profiles were retrieved from the study of Wang et al. for East Asia ([Wang et al., 2010](#)).

2.2. Air Quality and Meteorological Models

In this work, we adopted the state-of-the-science chemical transport model and the Community Multi-scale Air Quality (CMAQ) model v5.2 to simulate the distributions and the contributions of residential BC emissions from rural households in China in 2014 ([Byun and Schere, 2006](#)). Despite the chemically inert nature, BC emission contributions from rural residential emissions were resolved by subtracting a sensitivity experiment that excluded rural residential BC emission from the baseline simulation. Such a method retained the coagulation and coalescence processes of BC particles with other aerosol components.

The Weather Research and Forecasting (WRF) model ([Skamarock et al., 2008](#)) v3.8 provided hourly meteorological fields to drive the CMAQ simulations. The original USGS land cover information was updated by land-use datasets from CAS-REDCP ([Liu et al., 2014](#)). We derived the boundary and initial conditions for the air quality simulations from outputs of a global atmospheric chemistry model, GEOS-Chem ([Wang et al., 2004](#)). The performance of the chemistry transport model and the meteorological model was evaluated by comparing model outputs with available observations from ground-level monitoring stations in China. The results indicate that models could perform robust meteorological field and air pollutants distributions in this study. Note that the bias in the evaluation results was involved in the uncertainty assessments.

Rural residential BC emissions in China were developed and explicitly described in [Section 2.1](#), which has been recompiled to 27×27 km spatial resolution so as to merged with emission inventories from other sources. Emissions from other sources consist of anthropogenic emissions from the MEIC emission dataset ([Zhang et al., 2009](#)), biogenic emissions from the BEIS 3.61 model ([Fehsenfeld et al., 1992](#)), dust emissions from CMAQ built-in windblown dust emission module and biomass and waste burning emissions from the FINN v1.5 dataset ([Jiang et al., 2012](#)). These emission inventories were combined and conducted temporal allocations, vertical allocations, and speciation to construct a time-varying three-dimensional inventory for model simulations.

The statistical measures employed in this study to quantify our

model performance included normalized mean bias (NMB), normalized mean error (NME), root mean square error (RMSE), and correlation coefficient (r). The definition of each indicator is:

$$NMB = \frac{\sum_{i=1}^n (M_i - O_i)}{\sum_{i=1}^n O_i} \times 100\%, \quad (7)$$

$$NME = \frac{1}{n} \sum_{i=1}^n \frac{|M_i - O_i|}{O_i} \times 100\%, \quad (8)$$

$$RMSE = \left[\frac{1}{n} \sum_{i=1}^n (M_i - O_i)^2 \right]^{\frac{1}{2}}, \text{ and} \quad (9)$$

$$r = \frac{\sum_{i=1}^n (M_i - \bar{M}) \times (O_i - \bar{O})}{[\sum_{i=1}^n (M_i - \bar{M})^2 \times (O_i - \bar{O})^2]^{\frac{1}{2}}}, \quad (10)$$

where M is model predictions and O is observation measurements.

Baseline emission inventory contains emissions from major biogenic and anthropogenic emission sectors, including industry, power generation, transportation, and etc. Annual total emissions for each chemical specie or compound, as well as their source contributions, are summarized in Fig. 2. Note that the residential and commercial sector is the predominant emissions sources of BC, accounting for 49.5% of annual BC emissions. It also contributes a significant portion of OC, SO₂, and CO emissions.

Temporal allocation, chemical speciation, and vertical assignment were conducted to compile the model-ready inventory. The speciation was processed in accordance with the Carbon Bound (CB05tucl) gas-phase mechanism and Aerosol 6 (AE6) particle-phase mechanism framework. Temporal allocation and chemical speciation were executed in the same way with our previous exercise (Gu and Yim, 2016; Yim et al., 2019a). The emission inventory was ultimately configured to be hourly inventory at a 27 km spatial resolution with 26 vertical layers.

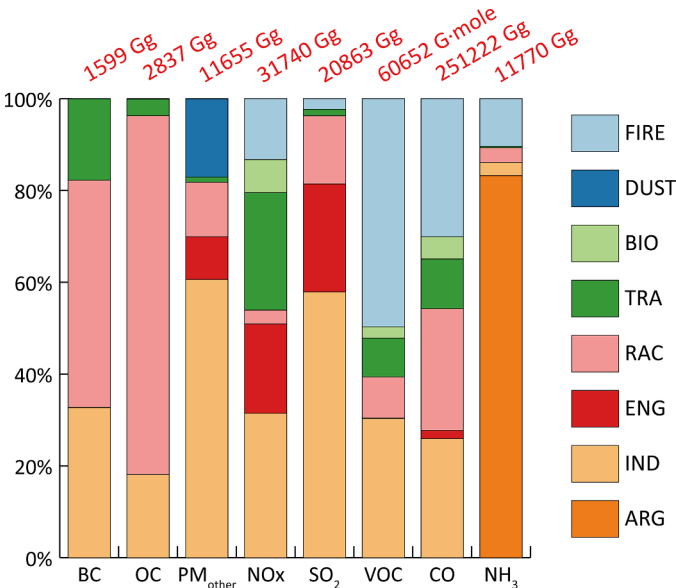


Fig. 2. Emission statistics of the baseline scenario for different chemical species and emission sectors. FIRE denotes to wildfire emissions; DUST denotes to wind-blown dust emissions; BIO denotes to emissions from biogenic sources; TRA refers to transportation emissions; RAC refers to residential and commercial emissions; ENG refers to emissions from power generation; IND is industrial emissions; ARG is emissions from agricultural fertilizer.

2.3. Process analysis

To explore the potential driving forces of the spatial-temporal distribution of BC concentrations, we integrated a process analysis module that apportions the transient BC concentration changes to different physicochemical processes together with the BC concentration simulation. The process analysis tool differentiated process contributions by operator splitting to different processes of species continuity equations in 3D space (Gipson, 1999). Such a method is expressed as follows:

$$C(t + \Delta t) - c(t) = \sum_{i=1}^n \int_t^{t+\Delta t} L_i dt \quad (11)$$

where $c(t)$ denotes the concentration level at time t ; Δt denotes the CMAQ time step; and L_i represents individual physicochemical processes. In practice, we tracked the BC concentration changes and apportion them to vertical advection and diffusion (ZADV and VDIF), horizontal advection and diffusion (HADV and HDIF), pollutant emissions (EMIS), dry deposition (DDEP), aerosol thermodynamic formation (AERO), and cloud process and wet deposition (CLDS). Note that dynamic processes were grouped into two clusters for easier discussion: ZADV and VDIF; EMIS and DDEP were lumped into physical processes in the vertical direction (VERT), and HADV and HDIF were combined as physical processes in the horizontal direction. Similar to the concentration impact, process analysis was conducted along with baseline and sensitivity simulations. The rural residential component was derived from the subtraction of these two simulations on the basis of the linear relationship of different processes considered in this study.

2.4. Human health impact

We applied the CRF derived from epidemiological research to estimate premature mortalities due to the exposure of rural residential populations to elevated BC concentrations. The function was adapted to firstly describe the all-cause mortalities under the exposure to annual ambient BC concentrations and then to extract that portion of the impact arising from rural residential emissions, which was determined by their BC concentration contributions. In the detailed calculation, premature mortalities under the exposure of ambient BC concentration were estimated by the combined effect of population, baseline incident rate, and the health risk factor that is linked in a log-linear relationship with the unit increase of BC concentration. RR-1 represents the additional health risk from BC concentration. The method is expressed as follows:

$$RR_k = e^{\gamma \cdot X_k} \quad (12)$$

$$E = \sum_k (RR_k - 1) / RR_k \cdot P_k \cdot f_k \quad (13)$$

where k refers to the grid index; P denotes to the population size that extracted from CAS-REDCP datasets (Xu, 2017); and f refers to the all-cause mortality rate above 30 years of age in 2014 based on the public health statistics of China (MOH, 2015). RR refers to relative risk and X_k denotes BC concentrations ($\mu\text{g}/\text{m}^3$). Note that a threshold concentration was not specified in this study, as evidence for no additional health risk below a certain BC concentration is currently inconclusive.

Regarding the value of the C-R coefficient (γ), our previous study has fitted CRF for PM_{2.5} concentrations specifically for China, and the majority of BC particles are subsets of PM_{2.5}. However, other studies have reported a higher health risk in response to the changes of BC concentration than PM_{2.5} compounds (Bell et al., 2009; Lipfert et al., 2006; Peng et al., 2009). Therefore, BC emitted from rural residential combustion may have a stronger association with human health. In this study, the values of coefficient γ were retrieved from a meta-regression that pooled all-cause mortalities to BC concentration from multiple cohorts (Achilleos et al., 2017). Note that Chinese samples were involved in this analysis to capture the health risk at the high BC concentration level.

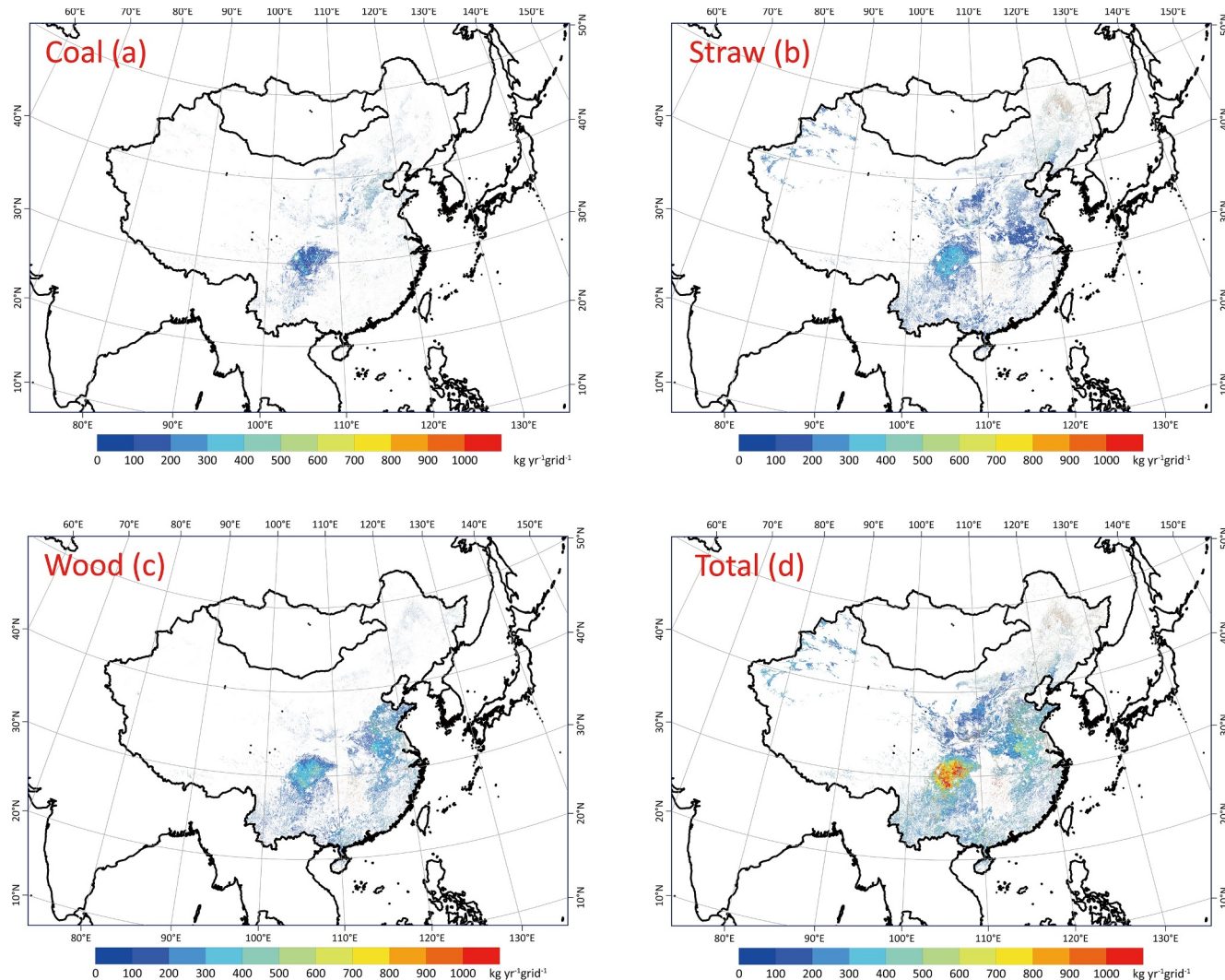


Fig. 3. Spatial distribution of rural residential BC emissions (kgBC/yr/grid) in China in 2014. The estimation results refer to the consumption of (a) coal, (b) straw, (c) wood, and (d) total solid fuel at 1×1 km grid resolution across rural China, where the total affected population is 7.09 billion, about 52% of the total population in China.

Table 1
Comparison of residential BC emission with other studies.

Studies	Source locations and year	Estimation method	Emissions (Gg/year)
Qin and Xie (2012)	Rural/Urban, 2009	BC emissions are calculated for counties and then allocated to $0.25^\circ \times 0.25^\circ$ grids	777.4
Wang et al. (2012)	Rural, 2007	BC emissions are calculated for 2373 counties and then allocated to $0.1^\circ \times 0.1^\circ$ grids	819.9
Wang et al. (2012)	Rural, 2014	Projected based on the emission inventory in 2007 and the fuel consumption trend from the National Long-term Development Plan (2008–2050)	697.7
Tao et al., (2018)	Rural, 2012	BC emissions are estimated based on EF and national energy consumption regressed by electricity consumption and some other impact factors	880.0
Zhao et al. (2013)	Rural/Urban, 2010	BC emissions are estimated based on EF and provincial energy consumption obtained from the Chinese official energy statistics	809.0
Lu et al. (2011)	Rural/Urban, 2010	BC emissions are estimated based on EF and provincial energy consumption provided by the International Energy Agency	936.0
Zhang et al. (2009)	Rural/Urban, 2006	BC emissions are estimated based on EF and provincial energy consumption provided by China Energy Statistical Yearbooks	1002.0
Streets et al. (2003)	Rural/Urban, 2000	Same as above	782.0
Zhang et al., 2018b	Rural, 2014	BC emissions are calculated for 33 provinces by extrapolation based on energy consumption and technology share among rural households	640.2
This work	Rural, 2014	Estimation of fuel consumption per household, EF _{BC} , the share of improved stoves and rural population density at 1×1 km grid	648.0

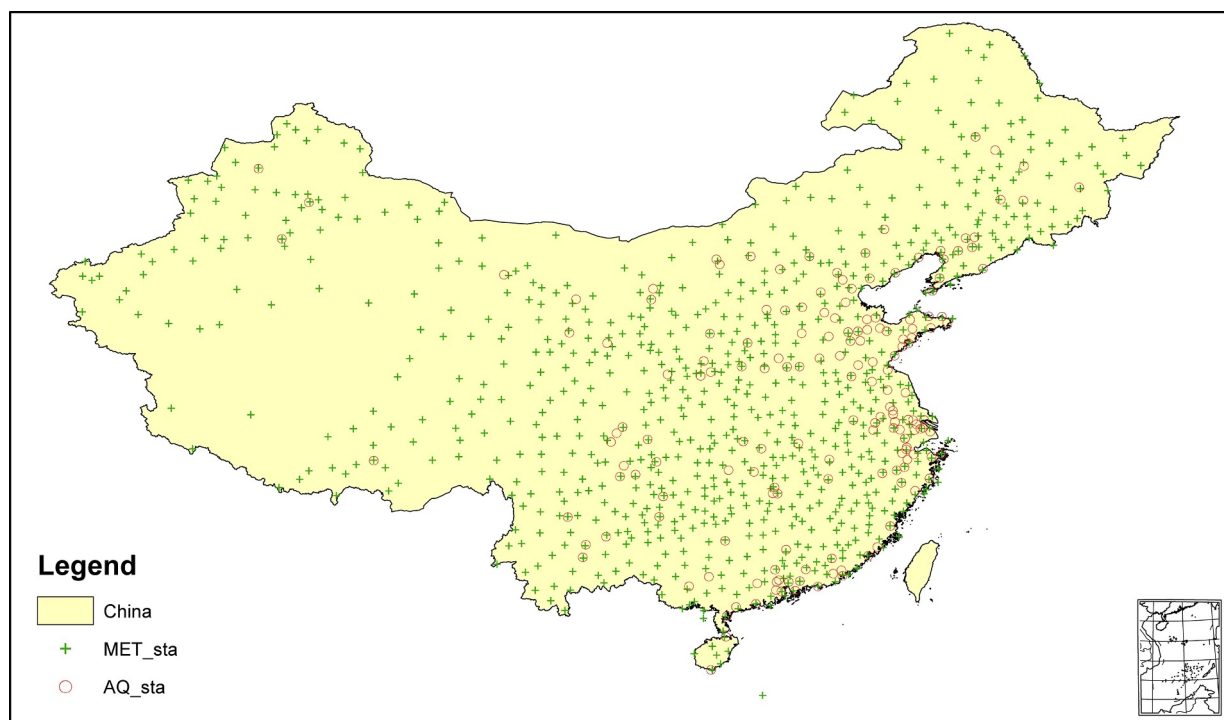


Fig. 4. Spatial distribution of surface meteorological stations (green cross mark) and air quality observations (red circle mark) in China. MET_sta refers to meteorological stations, where AQ_sta refers to air quality stations. (For interpretation of the references to color in this figure legend, the reader is referred to the web version of this article.)

2.5. Uncertainty assessment

We applied the Monte-Carlo approach to investigate the uncertainty range of our human health estimates (Yim et al., 2019b). The uncertainties may come from the accumulated variability of emission estimation of BC, the evaluation results of the air quality model, and the coefficients of CRFs. Specifically, the uncertainty of emission estimation was attributed to the coefficients' uncertainty, which is described in Section 2.1. To adjust the bias between model prediction and stationary observations, a factor of 1.04 [95%CI: (0.55, 3.48)], which was derived from the normalized mean bias (NMB) for all stations, has been applied to the annual BC concentrations. In terms of the health impact calculation, uncertainties were related to the coefficient γ of CRFs, the details of which are discussed in Section 2.4. All uncertainty factors were simulated 20,000 times, assuming a triangular probability distribution based on their median value and 95% confidential interval (CI). Each realization was input into the health impact estimation and a probability distribution constructed. The ultimate range of uncertainty was expressed by the median value and 95%CI of this distribution.

3. Results

3.1. Residential BC emissions in rural China

The gridded BC emissions at 1×1 km grid resolution from solid fuel consumption across rural households were produced based on the estimation of the share of improved stoves, emission factors (EF_{BC}), fuel consumption and rural population density. The spatial distribution of annual rural residential emissions and the breakdown for each fuel type are summarized in Fig. 3(a)-(d). The results show that the total BC emissions caused by solid fuel consumption by rural households were estimated to be 648.0 (95%CI: 361.0–965.9) gigagram (Gg) in 2014. Coal burning contributes 119.2 (95%CI: 92.9–128.6) Gg BC, accounting for 18.4% of the total. Straw burning contributes 302.9 (95%CI: 161.2–474.1) Gg BC, 46.7% of the total. Wood combustion contributes

247.5 (95%CI: 118.2–396.9) Gg BC, 38.2% of the total.

The highest residential BC emissions in rural areas are found in the Sichuan Basin, due to a large number of rural residents and the consequent substantial consumption of straw and wood. High emission densities are also found in North China and East China. According to the spatial distribution estimates, emissions in North China primarily come from the combustion of coal and straw, while emissions in East China are largely from wood and straw consumption. In addition, significant emissions are also found in Northeast China, Northwest China, and South China, which are predominantly derived from wood and straw combustion.

We compared our emissions inventory with estimations from other studies. The results are shown in Table 1. In general, the total BC emissions calculated in this study are lower than previous estimates. One possible reason could be the specification of stove technology in this study, which was derived from extensive field surveys and was not available in previous studies. We found that traditional techniques associated with higher emission factors were being phased out, while the increasing use of improved stove techniques has resulted in lower emission factors. Another factor could be the estimation of energy consumption. We calculated the detailed energy consumption for every individual household, which may not be accurately reflected in state-, provincial-, and county-level statistics that were used in previous research in Table 1.

3.2. Performance evaluations of meteorology and air quality model

The simulation results were evaluated with a substantial amount of ground-level observations. Specifically, simulated surface temperature, wind, and air pressure were compared with daily measurements from 823 surface meteorological stations in China. As the large-scale BC monitoring in China is lacking, the CMAQ model capacity in accurately simulating BC concentration was evaluated by comparing the simulated $PM_{2.5}$ with daily measurements from 171 surface air quality observation stations in China. The spatial distribution of these observation

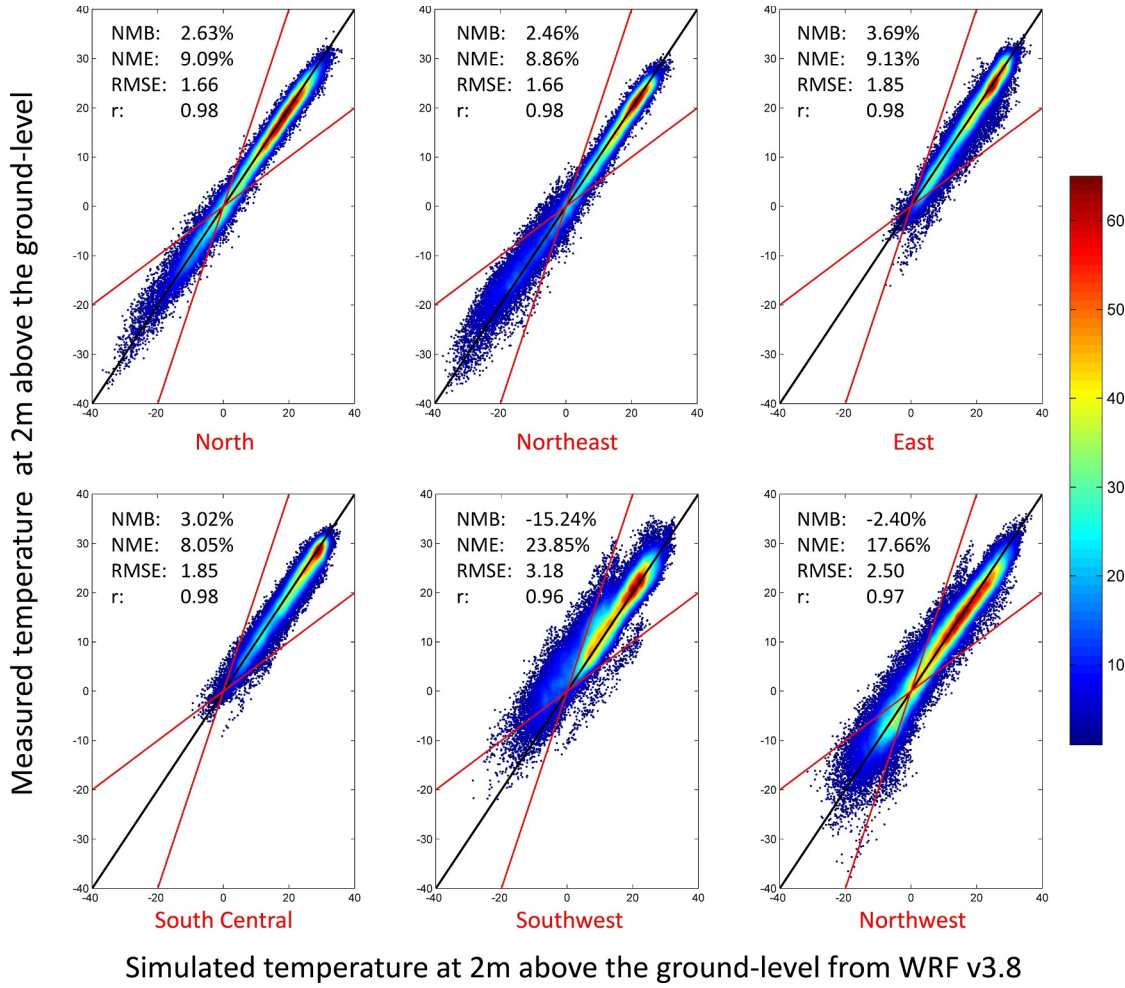


Fig. 5. Comparison between the simulated temperature at 2 m above the ground-level with 2 m temperature observed from meteorological observations. Black line indicates perfect prediction of temperature from WRF v3.8 model. Red lines represent the two times higher or lower prediction of temperature from WRF model. Rendered color shows the overlaid model-observations pairs. NMB, NME, RMSE, and r are the statistical indicators, representing normalized mean bias, normalized mean error, root mean square error, and correlation coefficient, respectively. (For interpretation of the references to color in this figure legend, the reader is referred to the web version of this article.)

stations is shown in Fig. 4.

Owing to the number of meteorological and air quality observation stations in China, the evaluation results for WRF v3.8 and CMAQ v5.2 were gathered and averaged by the six regions of China defined according to ISO 3166-2: CN (International Organization for Standardization, 2007), see Figs. 5–7. Fig. 5 shows that the model simulated temperature matches well with ground-level observations, especially in North China, Northeast China, East China, and South Central China. The averaged normalized mean bias, normalized mean error, root mean squared error, and correlation coefficients for these four regions are 2.95%, 8.78%, 1.76, and 0.98, respectively. The statistics also suggest a slight underestimation of temperature in these four regions. In contrast, the bias and error of model simulations against ground-level observations are relatively larger in Southwest China and Northwest China, which may be due to the complex topography in West China, as well as a few numbers of observations stations available. Similar findings and explanations are given in the previous modeling study (Yu et al., 2015). The statistics suggest a slight overprediction of temperature in these two regions.

The evaluation results of wind speed simulation as shown in Fig. 6 indicate that WRF v3.8 could capture the daily fluctuation of wind speed well at current spatial resolution in China. The averaged correlation coefficient in six regions in China is 0.68. On the other hand, averaged normalized mean bias and normalized mean error of wind

speed in six regions in China are 82.4% and 89.56%, suggesting an overestimation of wind speed. The causes of this overestimation could be the lack of involvement of urban effect on wind convergence. Such overestimation is more significant in the western part of China. The complex terrain in West China also increases the uncertainty of the model prediction.

CMAQv5.2 reproduced PM_{2.5} spatio-temporal distribution well in different regions in China, as shown in Fig. 7. The correlation coefficient and root mean square error averaged for different regions ranged from 0.67 to 0.71 and from 34.95 to 39.05, respectively. Among all regions, the simulated PM_{2.5} concentration was closer to the observations in the eastern and central China (North China, Northeast China, East China, and South Central China), mostly within the two times bias. The statistic results note an overall slight overestimation of PM_{2.5} simulation in these regions, probably is due to the overestimation of anthropogenic emissions or inaccurate size partition of total particulate matter. In the western China (Southwest China and Northwest China), CMAQ tended to produce PM_{2.5} lower than the ground-level observations. Such pattern occurred during the lower concentration episode in Southwest China and both lower and higher episode in Northwest China. Statistic results also report a slightly higher normalized mean error in the West China than the East and South Central China. Several factors may account for this underestimation. Firstly, the dust emission module inbuilt in the CMAQ model may not be able to fully regenerate

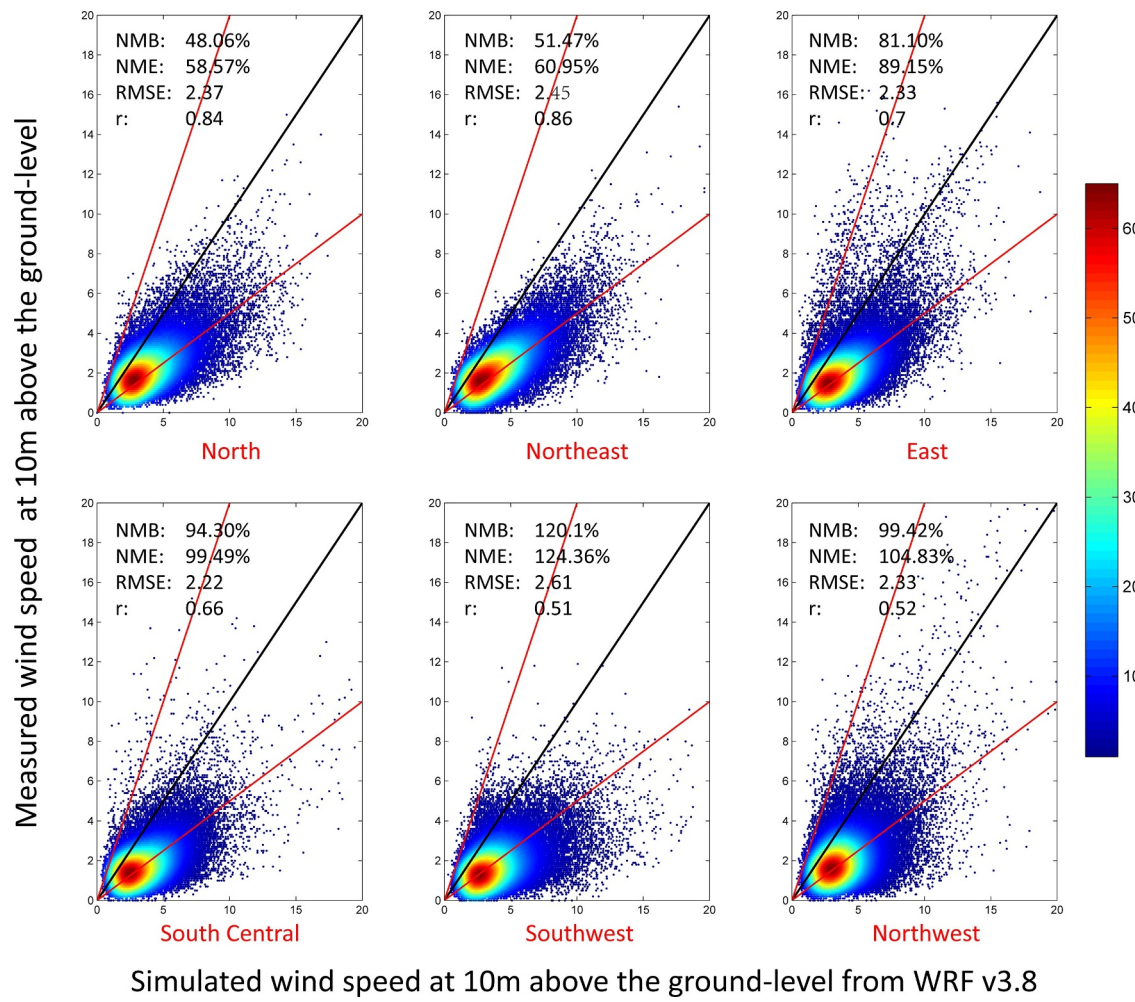


Fig. 6. Comparison between simulated horizontal wind speed at 10m above the ground-level with 10 m wind speed observed from meteorological observations. Black line indicates the perfect prediction of wind speed from WRF v3.8 model. Red lines represent the two times higher or lower prediction of wind speed from WRF model. Rendered color shows the overlaid model-observations pairs. NMB, NME, RMSE, and r are the statistical indicators, representing normalized mean bias, normalized mean error, root mean square error, and correlation coefficient, respectively. (For interpretation of the references to color in this figure legend, the reader is referred to the web version of this article.)

dust emissions in the Northwest China. Mountainous topography around Tibet Plateau and high elevation in the Southeast China increase the bias in meteorology reproduction, which is also discussed in the evaluation results of the meteorological model. This discrepancy would not significantly affect BC simulation results, as the rural domestic BC emissions in West China are fairly limited.

3.3. Spatio-temporal distribution of BC concentration impact

Fig. 8 depicts the spatial distribution of BC concentration due to residential emissions in the rural area of mainland China. Generally, residential BC emissions in the rural area contributed $0.65 \mu\text{g}/\text{m}^3$ annual mean BC concentration over China, accounting for 51.8% of total BC in China. Such impacts were more prominent in the rural areas with significant residential BC emissions, including Northeast China, North China, and the Sichuan Basin. The highest impact, as much as $11.53 \mu\text{g}/\text{m}^3$ annual mean BC, was found in the Sichuan Basin, which can be explained by the significant amount of residential BC emissions, the high rural population density, and the complex topography, which was unfavorable for the dispersion of air pollution. South China and West China were less affected by the residential emission impact in rural areas. To further clarify the physical and chemical mechanisms controlling the spatial distribution pattern, process analysis was applied to the urban and rural areas of four divisions with distinctive annual mean

BC concentration in China, as shown in the right panel of Fig. 8. Regional divisions were determined by k-means clustering of gridded annual BC concentration values from the model outputs. The resultant center values for the four divisions was found to be $[0.15, 1.23, 3.51, 8.46] \mu\text{g}/\text{m}^3$ for T1 to T4. Typical regional divisions are shown by black boxes in the left panel of Fig. 8.

Explicit clustering results are given in Fig. 9. T1 primarily represents the Sichuan Basin, where the contribution of vertical physical processes to the changes of BC concentration was negative for both rural and urban areas. In contrast, the horizontal physical processes contributed positively to the changes in BC concentration for both rural and urban areas. Such a sensitivity pattern suggests that high concentrations in T1 were mainly attributable to BC transported from other divisions and trapped in the basin region. The sensitivity patterns in T2 and T4 were similar. High positive sensitivity of vertical components in the rural area indicates that the major contributor to BC concentration was local residential emissions. Excessive emissions were also advected and diffused horizontally to other divisions. Cloud scavenging and wet deposition were also found to be important for BC sinking to the rural area. On the other hand, pollutant transport from rural to urban areas in T2 and T4 was negligible. In T3, cloud processes in rural areas exerted a more significant impact on pollutant removal than in the other divisions, probably due to its location in southern China with more frequent and intensive precipitation. In addition, the comparable scale of

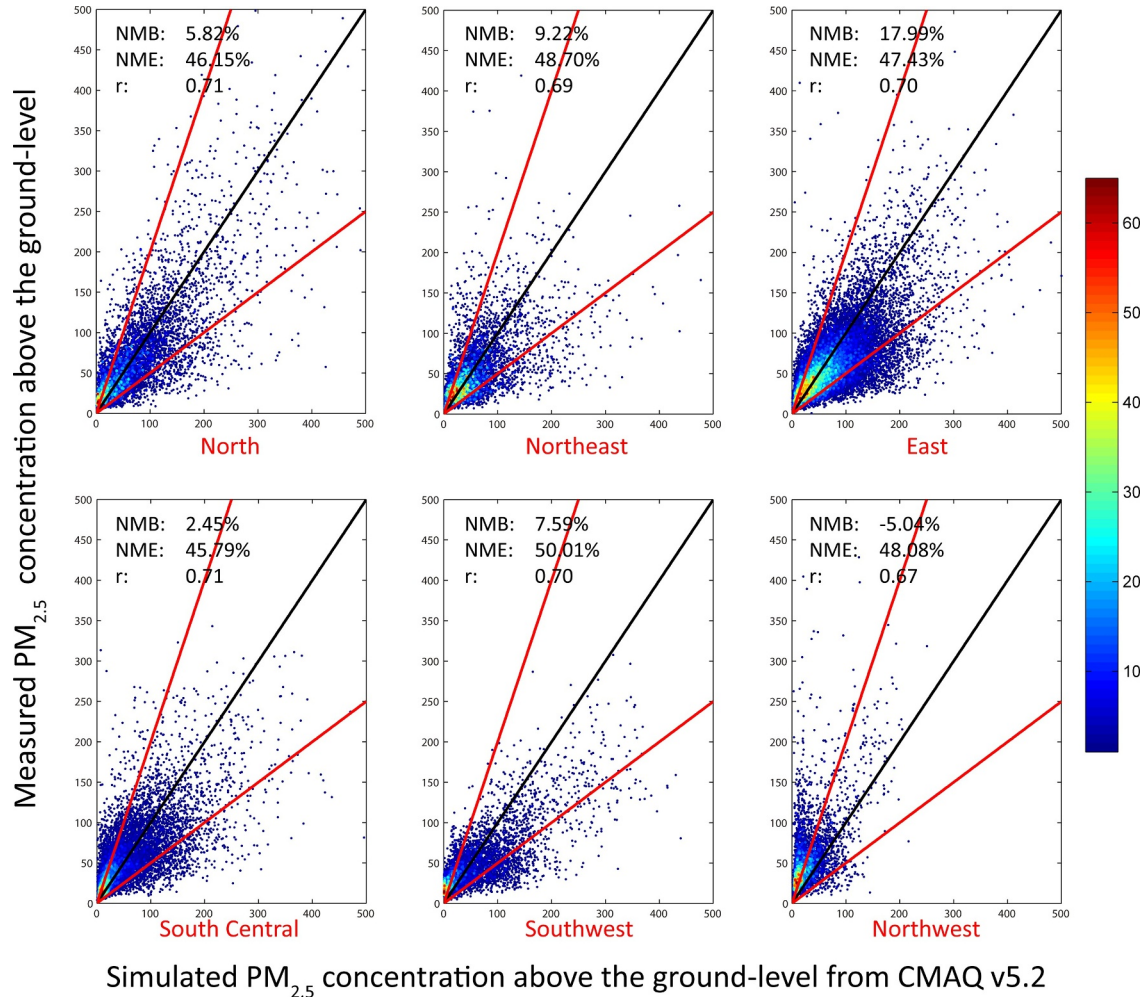


Fig. 7. Comparison between simulated PM_{2.5} concentration above the ground-level with corresponding PM_{2.5} concentration observed from air quality monitoring stations. Black line indicates the perfect prediction of PM_{2.5} from CMAQ v5.2 model. Red lines represent the two times higher or lower prediction of wind speed from WRF model. The rendered color shows the overlaid model-observations pairs. NMB, NME, RMSE, and r are the statistical indicators, representing normalized mean bias, normalized mean error, root mean square error, and correlation coefficient, respectively. (For interpretation of the references to color in this figure legend, the reader is referred to the web version of this article.)

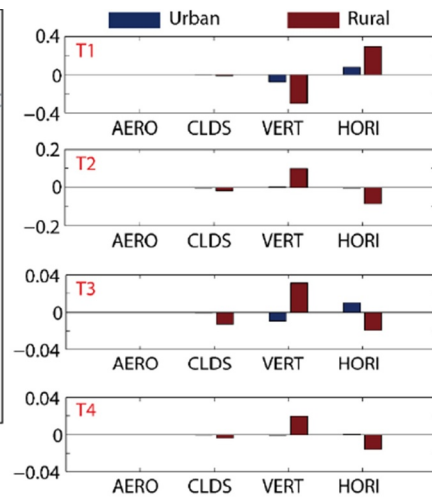
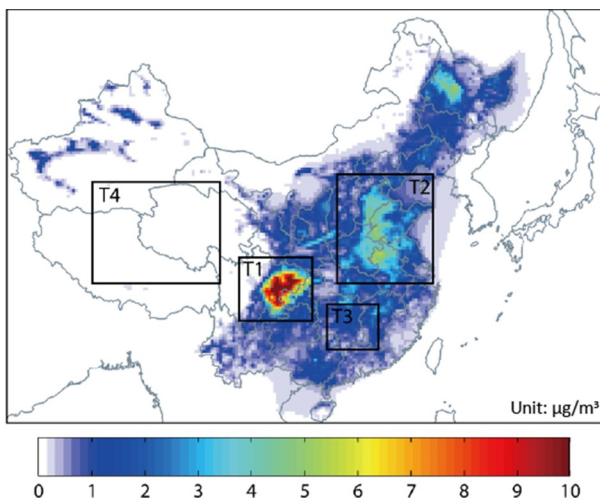


Fig. 8. The spatial distribution of BC concentration (left panel) and its sensitivity to various physical and chemical processes (right panel) due to residential emissions in the rural area of mainland China. Black boxes in the spatial distribution figure indicate samples of four divisions of BC concentration level. AERO, CLDS, VERT, and HORI refer to aerosol processes, cloud processes, vertical physical processes, and horizontal physical processes, respectively.

horizontal physical processes in rural and urban areas in T3 reflected the presence of BC transport from rural to urban areas.

In terms of temporal variation, as shown in Fig. 10(a), the BC concentration impacts in the rural area were significantly higher in

winter due to the dramatic rise of energy consumption for residential heating. The statistics indicate that the averaged BC impacts over China were ranged from 0.34 $\mu\text{g}/\text{m}^3$ in July to 1.31 $\mu\text{g}/\text{m}^3$ in January. As regards diurnal variation, higher BC concentration impacts were found

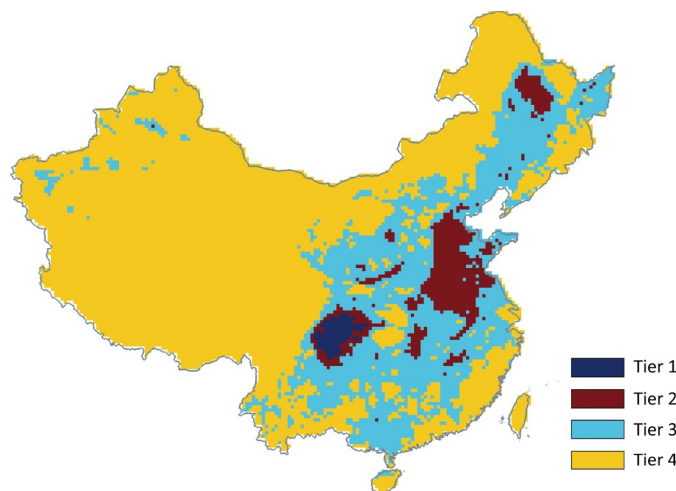


Fig. 9. Divisions of annual BC concentration due to the domestic emissions in the rural area of China, based on k-means clustering of gridded concentration value.

during the nighttime (18:00–8:00), while a lower impact occurred in the afternoon (12:00 – 14:00). Our results show that the BC concentration impact reached its highest value of $1.16 \mu\text{g}/\text{m}^3$ at 22:00 and dropped to its lowest level of $0.24 \mu\text{g}/\text{m}^3$ at 13:00 averaged over China. Fig. 10 (a) also identifies more prominent BC impacts in urban areas in winter than summer, while the hourly variation was weaker. To further elucidate the reasons for these temporal variation patterns, we applied process analysis for urban and rural receptor regions. The results are depicted in Fig. 10(b–e). Our process analysis results indicate that AERO contributed only marginally to the impact of BC concentrations arising from rural residential emissions. CLDS effects in BC removal was more prominent in rural areas, which are described in Fig. 10(c). Cloud processes and wet deposition were more effective at removing BC during the summer and night time when there was abundant moisture in the atmosphere. Cloud processes were thus expected to decrease the BC concentration, in particular during the period from 17:00 to 8:00 from June–September in the rural areas. On the contrary, CLDS signal was found in wintertime in the urban area. The difference seasonal pattern may be associated with the seasonal pattern of BC concentration in urban areas, which was the source origin of cloud removal. VERT was found to have a stronger impact on BC concentration arising from rural residential emissions, as shown in Fig. 4 (d). In rural areas, positive VERT from 14:00– 22:00 led to the accumulation of BC aerosol and contributed to the highest BC concentrations occurring at 22:00. The concentration was then found to decrease until 13:00, which was consistent with the period of negative VERT. Positive VERT was mainly attributable to the residential emissions generated by cooking and heating activities in the evening. In the nighttime, without significant emission activity, pollutants removal acted as a dominant role in VERT process. The strongest removal process was identified in the morning, even up to the level to cancel out contributions of local emissions. Such divergence was more prominent in the winter. On the other hand, VERT contributed to overall negative impacts in urban areas, and was higher in winter and nighttime. Hori impacts in the urban areas show a similar but opposite variation pattern, suggesting that the potential source of vertical removal was BC accumulation from significant horizontal transportation in the nighttime. In terms of Hori process, rural and urban areas show a similar but opposite temporal variation of Hori contributions to BC concentration due to rural residential emissions. In urban areas, significant contribution signals were found in winter and nighttime, during which higher concentration impact were also presented in rural areas. This pattern suggests that the higher Hori contribution may be associated with larger BC concentration differences between the rural and urban area in winter and nighttime, together

with regional air movement that advected and diffused BC from rural to the urban area. Such mechanism also supports the understanding of BC transportation between the rural and urban areas in T3.

3.4. Human health impact

Residential BC emissions from the rural area of China were estimated to induce 171,000 [95%CI (69,000, 387,000)] premature mortalities in China. Based on the spatial distribution shown in Fig. 11, the most significant health impacts occurred in the Sichuan Basin and in East China, while lower impacts were found in West and North China.

We summarized the health impacts in different provinces and further classified them into rural and urban regions, as shown in Fig. 12. Sichuan [37,000 (95%CI: 33,000–46,000)], Henan [18,000 (95%CI: 16,000–23,000)], and Shandong [18,000 (95%CI: 14,000–26,000)] were the top three provinces that received the highest mortalities from rural BC emissions, together accounting for 43.2% of the total impacts in China. Most of these health impacts occurred in rural areas that were close to the emission sources, in particular for those economically underdeveloped provinces. The health impacts in rural areas of Gansu, Yunnan, Guizhou, Guangxi, Jilin, Jiangxi, Heilongjiang, Hainan, and Tibet regions were approximately 10 times higher than in the urban areas. Major metropolitan areas (for example, Shanghai, Beijing, and Tianjin) were also identified to have health impacts, predominantly in the urban areas due to the dense population. These differences with other provinces could be attributable to the significant UHI effect in metropolitan areas that enhanced the transport of BC particles from rural to urban areas during nighttime, which has been observed in Zheng et al., 2018. The large coverage of the built-up area with a dense population can be another contributor to this variance.

4. Conclusions and discussions

Residential BC emissions and concentrations from rural areas show a different distribution pattern than other aerosol components. The peak PM concentrations in North China were recognized by both modeling simulation (Hu et al., 2017; Ning et al., 2018; Zheng et al., 2017) and satellite retrieval methods in recent decades (He and Huang, 2018; Ma et al., 2014; Wang et al., 2019). We found the highest BC concentration in the Sichuan Basin. Local emissions and significant pollutant transferred from the surrounding area were responsible for the high concentration in this region. Basin topography further reduced the efficiency of pollutant dispersion. Such effect has been systematically assessed by an observational study (Ning et al., 2019). This work applied a process analysis method to support this hypothesis. Following the enforcement of strong emission control policies in three city agglomerations: the Beijing-Tianjin-Hebei (BTH) in north China, the Yangtze River Delta (YRD) region in east China, and the Pearl River Delta (PRD) region in south China, air pollution levels in these regions have been significantly declined, which gave prominence to the air pollution problem in the Sichuan Basin.

In this work, we adapted a concentration-response function specific for estimating health impacts of BC. The conversion factors from BC concentration to the relative risk of all-cause mortality (C-R) were derived from the meta-regression of a number of cohorts, among which studies were conducted in China, U.S. and E.U. Such regression conclusion may not be able to fully describe the BC concentration-risk relationship in China. Owing to the availability of BC observations, some cohorts derived BC concentration by assuming a fixed portion of PM or PM mixture with high BC fractions, like “black smoke”. Such assumptions may also increase the uncertainty in health impact estimation. The central estimations indicate that residential BC emissions in rural China caused 171,000 premature mortalities in 2014, slightly below the estimates provided in previous research made on the basis of $\text{PM}_{2.5}$ exposure, which were among 0.25–0.34 million mortalities during 2010–2013, (Archer-Nicholls et al., 2016; Gu et al., 2018; Hu et al.,

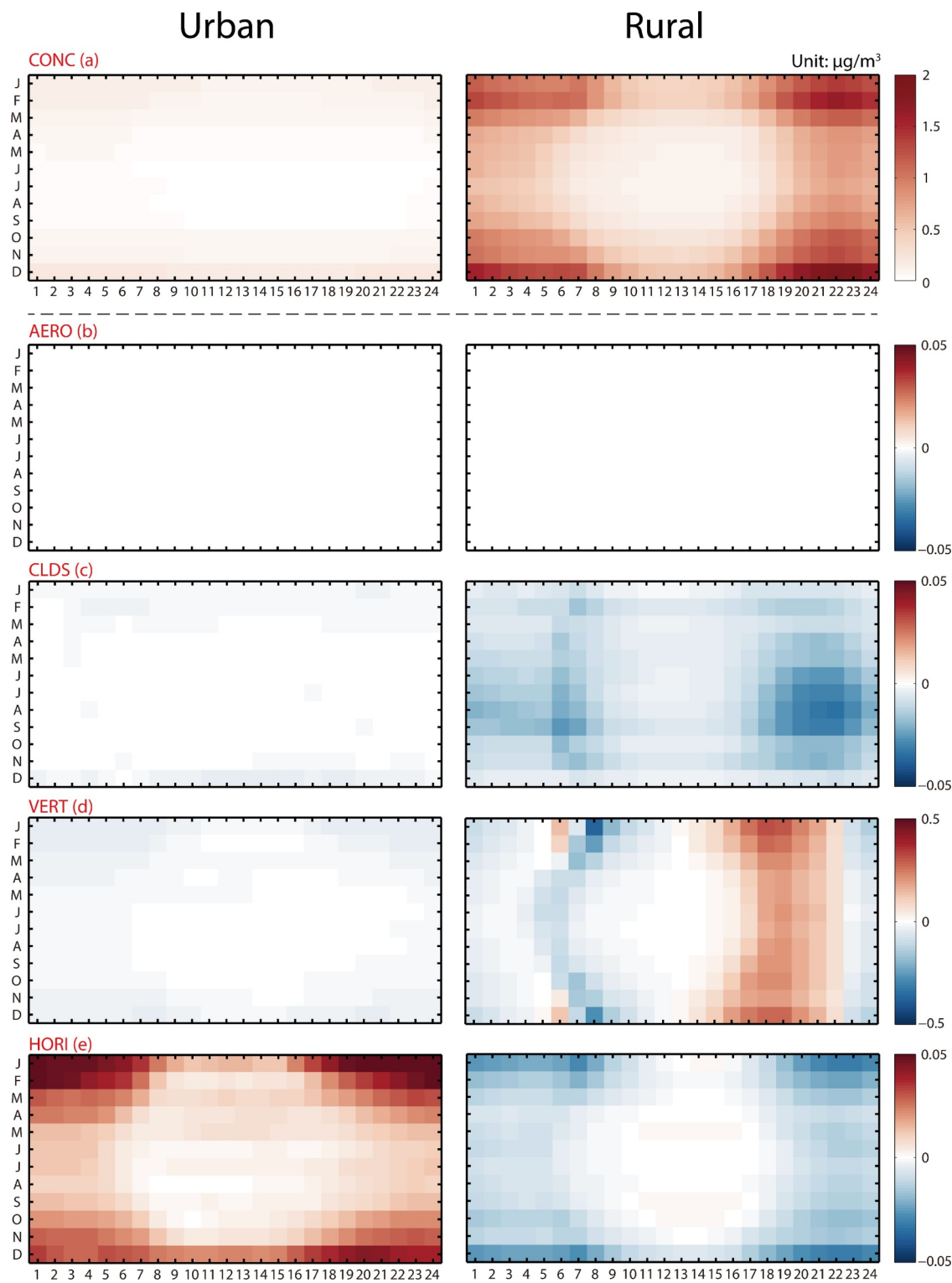


Fig. 10. The monthly and hourly variation of BC concentration due to residential emissions in the rural areas of mainland China. The abbreviations are as follows: CONC refers to BC concentration. AERO, CLDS, VERT, and HORI refer to aerosol processes, cloud processes, and physical processes in the vertical direction, and physical processes in the horizontal direction, respectively. The x- and y-axis of each subfigure denote the scales of hour and month, respectively. Units of all subfigures are $\mu\text{g}/\text{m}^3$.

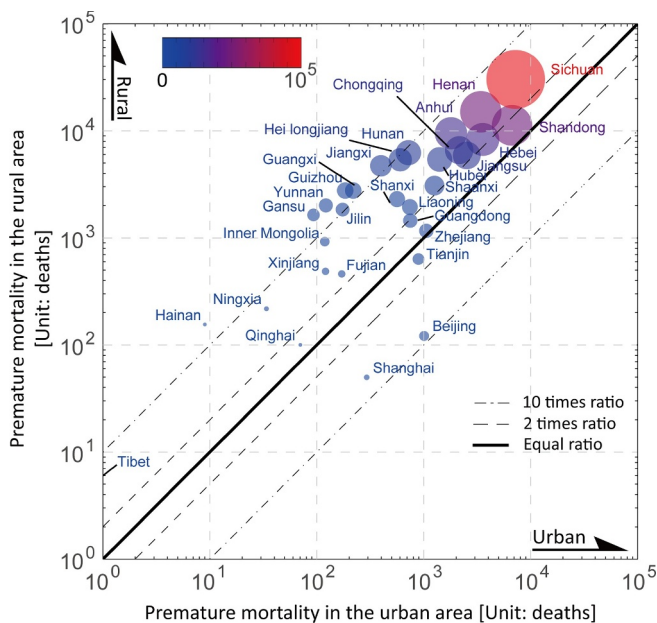


Fig. 11. Spatial distribution of annual premature mortalities due to rural residential BC emissions in China.

2017). This discrepancy is mainly derived from the specific focus of BC species out of PM_{2.5} mixture and rural region out of whole China, suggesting a reasonable range of health impacts in this study. BC-specific CRF functions are still limited. To constrain this large uncertainty, more epidemiological investigations are needed to fill the gap in the relationship between human health risk and exposure to BC.

This study comprehensively investigated rural residential BC from emissions to air concentration and the resultant impacts on premature mortality. When compared with the MEIC emission inventory, rural residential BC was found to contribute 40.6% of the annual BC emissions in China (1598.02 Gg) (Zhang et al., 2009). Our previous work

also highlighted the importance of residential and industrial emissions in the formation of PM_{2.5} (Gu et al., 2018). To mitigate the air pollution problem, the Chinese government has taken a series of efforts to reduce pollutant emissions in recent decades. Most of these measures focused on industrial, power generation, and vehicular emissions, such as the installation of desulfurization devices and the raising of vehicle emission standards (Huang et al., 2017; Q. Zhang et al., 2019; W. Zhang et al., 2019). Because of these emission reductions, the contributions of residential emissions to total pollution levels can be expected to increase in future (Yang and Teng, 2018; Zhang et al., 2017). Low-quality fuels are still extensively used in rural China, the combustion of which releases large amounts of carbonaceous pollutants. This study was designed to provide a systematic overview of the residential emission impact from rural areas of China, focusing on BC, an emission species that have the greatest health risk and also contributes to climate forcing (Liu et al., 2018, 2020; Yang et al., 2020). Our study is anticipated to provide a valuable foundation for the development of new pollution control measures for the residential sector to accompany the existing measures for the industrial, power generation and transportation sectors.

In current days, biomass fuels still act as the dominant energy source for cooking and heating in the rural areas of the developing countries (Zhang et al., 2018c). Recent studies found that BC emissions have significant contributions to PM_{2.5} concentration in the developing world (Anenberg et al., 2011; Philip et al., 2014). While residential energy uses in the developing regions, including Russia, Africa, Middle East, and India were found to account for more than 50% of black carbon emissions, higher than the value in China (Anenberg et al., 2011; Kumar et al., 2015). Meanwhile, individual exposure to residential BC would be even higher if exposures in indoor environments are also taken into account. People in rural areas often live in an environment with traditional stoves and poor ventilation, which is unfavorable for pollutants dispersion (Anenberg et al., 2013; Du et al., 2017; WHO, 2012). Therefore, residential BC emissions should have induced health outputs in the developing world. This study elucidated a comprehensive method that quantifying the ambient impact of BC emissions in China, from fuel consumption to health impact

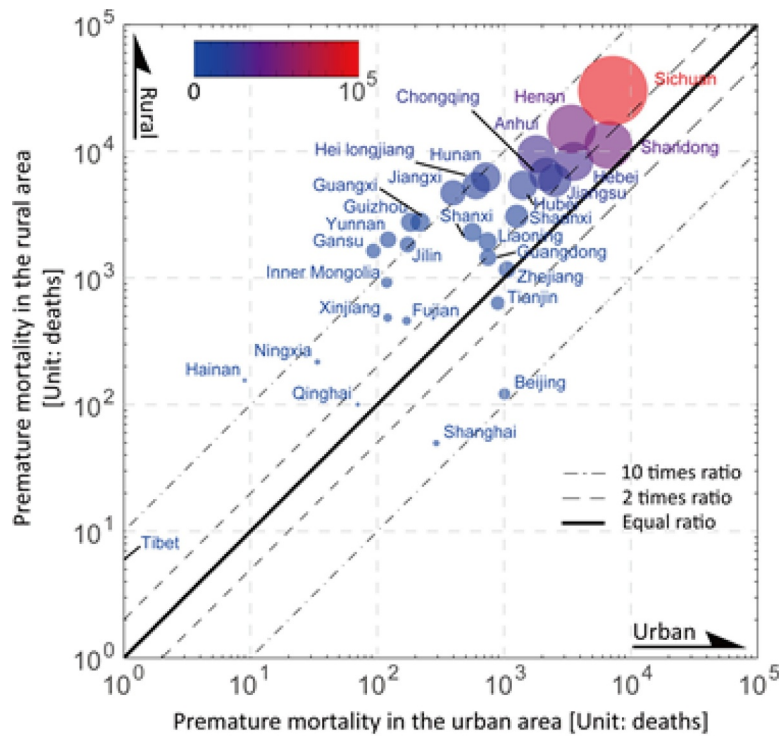


Fig. 12. Annual premature mortalities in urban and rural areas of different provinces due to rural residential BC emissions in China. X-axis and Y-axis describe the mortality in urban and rural areas on a logarithmic scale. Marker size and color linearly represent the uncertainty of premature mortality estimation in the corresponding province. The solid line reflects equal mortalities in the rural and urban area. The dashed line and the dot-dash line enclose the region with mortality ratio of rural and urban within 2 and 10 times, respectively.

estimations, which is also feasible to access the residential emission impacts in other countries. Such understanding is expected to be a valuable reference for enacting emission control measures in consideration of local energy structure.

CRediT authorship contribution statement

Yefu Gu: Conceptualization, Methodology, Writing - original draft.
Weishi Zhang: Conceptualization, Methodology, Writing - original draft.
Yuanjian Yang: Visualization, Methodology.
Can Wang: Software, Visualization.
David G. Streets: Supervision, Writing - review & editing.
Steve Hung Lam Yim: Conceptualization, Methodology.

Declaration of Competing Interest

The authors declare no competing financial interests.

Acknowledgments

This work is jointly funded by the Improvement on Competitiveness in Hiring New Faculties Fund (2013/14) of the Chinese University of Hong Kong; the Vice-Chancellor's Discretionary Fund of the Chinese University of Hong Kong (grant no. 4930744), the Early Career Scheme of Research Grants Council of Hong Kong (grant no. ECS-24301415), and National Key Research and Development Programme of China (National Key R&D Program of China), Social and economic costs of carbon emissions and reductions, under Contract number: 2016YFA0602500. Emission generation work was performed at Argonne National Laboratory under the support of the Office of Biological and Environmental Research in the U.S. Department of Energy (U.S. DOE), Office of Science. Argonne National Laboratory is operated by UChicago Argonne, LLC, under Contract No. DE-AC02-06CH11357 with U.S. DOE.

We would like to thank the National Meteorological Information Center, National Environmental Monitoring Center, Data Center for Resources and Environmental Sciences, Chinese Academy of Sciences, and NOAA's National Geophysical Data Center for providing meteorological, air quality, geographical, and nighttime light data, respectively. We acknowledge the support of the CUHK Central High Performance Computing Cluster, on which computation in this work has been performed.

The anthropogenic emissions inventory was retrieved from the open data at <http://www.meicmodel.org/>. The land cover and spatial-distributed population information are available at <http://www.resdc.cn/>. Meteorological and air quality observations at ground-level in China were derived from National Meteorological Information Center (<http://data.cma.cn/data/detail/dataCode/A.0012.0001.html>) and National Environmental Monitoring Center (<http://106.37.208.233:20035>

Supplementary materials

Supplementary material associated with this article can be found, in the online version, at [doi:10.1016/j.resconrec.2020.104812](https://doi.org/10.1016/j.resconrec.2020.104812).

References

- Achilleos, S., Kioumourtzoglou, M.A., Wu, C.Da, Schwartz, J.D., Koutrakis, P., Papapetropoulos, S.I., 2017. Acute effects of fine particulate matter constituents on mortality: a systematic review and meta-regression analysis. Environ. Int. <https://doi.org/10.1016/j.envint.2017.09.010>.
- Anderson, J.O., Thundiyil, J.G., Stolbach, A., 2012. Clearing the air: a review of the effects of Particulate matter air pollution on human health. J. Med. Toxicol. <https://doi.org/10.1007/s13181-011-0203-1>.
- Anenberg, S.C., Balakrishnan, K., Jetter, J., Masera, O., Mehta, S., Moss, J., Ramanathan, V., 2013. Cleaner cooking solutions to achieve health, climate, and economic co-benefits. Environ. Sci. Technol. <https://doi.org/10.1021/es304942e>.
- Anenberg, S.C., Talgo, K., Arunachalam, S., Dolwick, P., Jang, C., West, J.J., 2011. Impacts of global, regional, and sectoral black carbon emission reductions on surface air quality and human mortality. Atmos. Chem. Phys. 11, 7253–7267. <https://doi.org/10.5194/acp-11-7253-2011>.
- Archer-Nicholls, S., Carter, E., Kumar, R., Xiao, Q., Liu, Y., Frostad, J., Forouzanfar, M.H., Cohen, A., Brauer, M., Baumgartner, J., Wiedinmyer, C., 2016. The regional impacts of cooking and heating emissions on ambient air quality and disease burden in China. Environ. Sci. Technol. <https://doi.org/10.1021/acs.est.6b02533>.
- Bell, M.L., Ebisu, K., Peng, R.D., Samet, J.M., Dominici, F., 2009. Hospital admissions and chemical composition of fine particle air pollution. Am. J. Respir. Crit. Care Med. <https://doi.org/10.1164/rccm.200808-1240OC>.
- Bond, T.C., Doherty, S.J., Fahey, D.W., Forster, P.M., Berntsen, T., DeAngelo, B.J., Flanner, M.G., Ghan, S., Kärcher, B., Koch, D., Kinne, S., Kondo, Y., Quinn, P.K., Sarofim, M.C., Schultz, M.G., Schulz, M., Venkataraman, C., Zhang, H., Zhang, S., Bellouin, N., Guttikunda, S.K., Hopke, P.K., Jacobson, M.Z., Kaiser, J.W., Klimont, Z., Lohmann, U., Schwarz, J.P., Shindell, D., Storelvmo, T., Warren, S.G., Zender, C.S., 2013. Bounding the role of black carbon in the climate system: a scientific assessment. J. Geophys. Res. Atmos. <https://doi.org/10.1002/jgrd.50171>.
- Byun, D., Schere, K.L., 2006. Review of the governing equations, computational algorithms, and other components of the models-3 community multiscale air quality (CMAQ) modeling system. Appl. Mech. Rev. 59, 51. <https://doi.org/10.1115/1.2128636>.
- Chen, Y., Zhi, G., Feng, Y., Liu, D., Zhang, G., Li, J., Sheng, G., Fu, J., 2009. Measurements of black and organic carbon emission factors for household coal combustion in China: implication for emission reduction. Environ. Sci. Technol. <https://doi.org/10.1021/es9021766>.
- Cohen, A.J., Brauer, M., Burnett, R., et al., 2017. Estimates and 25-year trends of the global burden of disease attributable to ambient air pollution: an analysis of data from the Global Burden of Diseases Study 2015. The Lancet 389 (10082). [https://doi.org/10.1016/S0140-6736\(17\)30505-6](https://doi.org/10.1016/S0140-6736(17)30505-6).
- Du, W., Shen, G., Chen, Y., Zhu, X., Zhuo, S., Zhong, Q., Qi, M., Xue, C., Liu, G., Zeng, E., Xing, B., Tao, S., 2017. Comparison of air pollutant emissions and household air quality in rural homes using improved wood and coal stoves. Atmos. Environ. 166, 215–223. <https://doi.org/10.1016/j.atmosenv.2017.07.029>.
- Fehsenfeld, F., Calvert, J., Fall, R., Goldan, P., Guenther, A.B., Hewitt, C.N., Lamb, B., Liu, S., Trainer, M., Westberg, H., Zimmerman, P., 1992. Emissions of volatile organic compounds from vegetation and the implications for atmospheric chemistry. Global Biogeochem. Cycles. <https://doi.org/10.1029/92GB02125>.
- Gipson, G., 1999. Science Algorithms of the EPA Models-3 Community Multiscale Air Quality (CMAQ) Modeling System: Chapter 16, Process Analysis. Report No EPA/600/R-99/30; US Environmental Protection Agency, Office of Research and Development.
- Gu, Y., Wong, T.W., Law, C.K., Dong, G.H., Ho, K.F., Yang, Y., Yim, S.H.L., 2018. Impacts of sectoral emissions in China and the implications: air quality, public health, crop production, and economic costs. Environ. Res. Lett. <https://doi.org/10.1088/1748-9326/aad138>.
- Gu, Y., Yim, S.H.L., 2016. The air quality and health impacts of domestic trans-boundary pollution in various regions of China. Environ. Int. 97. <https://doi.org/10.1016/j.envint.2016.08.004>.
- He, Q., Huang, B., 2018. Satellite-based mapping of daily high-resolution ground PM2.5 in China via space-time regression modeling. Remote Sens. Environ. <https://doi.org/10.1016/j.rse.2017.12.018>.
- Highwood, E.J., Kinniswells, R.P., 2006. When smoke gets in our eyes: the multiple impacts of atmospheric black carbon on climate, air quality and health. Environ. Int. <https://doi.org/10.1016/j.envint.2005.12.003>.
- Hu, J., Huang, L., Chen, M., Liao, H., Zhang, H., Wang, S., Zhang, Q., Ying, Q., 2017. Premature mortality attributable to particulate Matter in China: source contributions and responses to reductions. Environ. Sci. Technol. <https://doi.org/10.1021/acs.est.7b03193>.
- Huang, L., Hu, J., Chen, M., Zhang, H., 2017. Impacts of power generation on air quality in China—part I: an overview. Resour. Conserv. Recycl. <https://doi.org/10.1016/j.resconrec.2016.04.010>.
- International Organization for Standardization, 2007. Codes for the representation of names of countries and their subdivisions.
- Imhoff, M.L., Lawrence, W.T., Stutzer, D.C., Elvidge, C.D., 1997. A technique for using composite DMSP/OLS "City Lights" satellite data to map urban area. Remote Sens. Environ. 61, 361–370. [https://doi.org/10.1016/S0034-4257\(97\)00046-1](https://doi.org/10.1016/S0034-4257(97)00046-1).
- Janssen, N.A.H., Hoek, G., Simic-Lawson, M., Fischer, P., van Bree, L., Brink, H., Ten, Keulen, M., Atkinson, R.W., Ross Anderson, H., Brunekreef, B., Cassee, F.R., 2011. Black carbon as an additional indicator of the adverse health effects of airborne particles compared with pm10 and pm2.5. Environ. Health Perspect. <https://doi.org/10.1289/ehp.1003369>.
- Jiang, X., Wiedinmyer, C., Carlton, A.G., 2012. Aerosols from fires: an examination of the effects on ozone photochemistry in the Western United States. Environ. Sci. Technol. <https://doi.org/10.1021/es301541k>.
- Jin, Y., Andersson, H., Zhang, S., 2016. Air pollution control policies in China: a retrospective and prospects. Int. J. Environ. Res. Public Health. <https://doi.org/10.3390/ijerph13121219>.
- Krewski, D., Jerrett, M., Burnett, R.T., Ma, R., Hughes, E., Shi, Y., Turner, M.C., Pope, C.A., Thurston, G., Calle, E.E., Thun, M.J., Beckerman, B., DeLuca, P., Finkelstein, N., Ito, K., Moore, D.K., Newbold, K.B., Ramsay, T., Ross, Z., Shin, H., Tempalski, B., 2009. Extended follow-up and spatial analysis of the American Cancer Society study linking particulate air pollution and mortality. Res. Rep. Health. Eff. Inst. [https://doi.org/10.1002/\(SICI\)1096-8652\(199905\)61:1<1::AID-AJH1>3.0.CO;2-J](https://doi.org/10.1002/(SICI)1096-8652(199905)61:1<1::AID-AJH1>3.0.CO;2-J).
- Kumar, R., Barth, M.C., Nair, V.S., Pfister, G.G., Suresh Babu, S., Sathesh, S.K., Krishna Moorthy, K., Carmichael, G.R., Lu, Z., Streets, D.G., 2015. Sources of black carbon aerosols in South Asia and surrounding regions during the integrated campaign for

- aerosols. *Gases Radiat. Budg. (ICARB). Atmos. Chem. Phys.* <https://doi.org/10.5194/acp-15-5415-2015>.
- Li, B., Gasser, T., Ciais, P., Piao, S., Tao, S., Balkanski, Y., Hauglustaine, D., Boisier, J.-P., Chen, Z., Huang, M., Li, L.Z., Li, Y., Liu, H., Liu, J., Peng, S., Shen, Z., Sun, Z., Wang, R., Wang, T., Yin, G., Yin, Y., Zeng, H., Zeng, Z., Zhou, F., 2016. The contribution of China's emissions to global climate forcing. *Nature* 531, 357–361. <https://doi.org/10.1038/nature17165>.
- Lim, S., Kim, J., Kim, T., Lee, K., Yang, W., Jun, S., Yu, S., 2012. Personal exposures to PM 2.5 and their relationships with microenvironmental concentrations. *Atmos. Environ.* <https://doi.org/10.1016/j.atmosenv.2011.10.043>.
- Lipfert, F., Baty, J., Miller, J., Wyzga, R., 2006. PM2.5 constituents and related air quality variables as predictors of survival in a cohort of U.S. military veterans. *Inhal. Toxicol.* <https://doi.org/10.1080/08958370600742946>.
- Li, J., Kuang, W., Zhang, Z., Xu, X., Qin, Y., Ning, J., Zhou, W., Zhang, S., Li, R., Yan, C., Wu, S., Shi, X., Jiang, N., Yu, D., Pan, X., Chi, W., 2014. Spatiotemporal characteristics, patterns and causes of land use changes in China since the late 1980s. *Dili Xuebao/Acta Geogr. Sin.* 69, 3–14. <https://doi.org/10.11821/dlxb201401001>.
- Liu, Z., Ming, Y., Zhao, C., Lau, N.C., Guo, J., Bollasina, M., Yim, S.H.L., 2020. Contribution of local and remote anthropogenic aerosols to a record-breaking torrential rainfall event in Guangdong Province, China. *Atmospheric Chemistry and Physics* 20, 223–241. <https://doi.org/10.5194/acp-20-223-2020>.
- Liu, Z., Yim, S.H.L., Wang, C., Lau, N.C., 2018. The Impact of the Aerosols Direct Radiative Forcing on Deep Convection and Air Quality in the Pearl River Delta Region. *Geophysical Research Letters* 45 (9), 4410–4418. <https://doi.org/10.1029/2018GL077517>.
- Lu, Z., Zhang, Q., Streets, D.G., 2011. Sulfur dioxide and primary carbonaceous aerosol emissions in China and India, 1996–2010. *Atmos. Chem. Phys.* <https://doi.org/10.5194/acp-11-9839-2011>.
- Ma, Z., Hu, X., Huang, L., Bi, J., Liu, Y., 2014. Estimating ground-level PM2.5 in China using satellite remote sensing. *Environ. Sci. Technol.* <https://doi.org/10.1021/es5009399>.
- MOH, 2015. *China Public Health Statistical Yearbook*. Beijing978-7-81136-536-8.
- National Bureau of statistics of China, 2015. *China Statistical Yearbook. China Statistical Yearbook*.
- Ning, G., Wang, S., Yim, S.H.L., Li, J., Hu, Y., Shang, Z., Wang, Jinyan, Wang, Jiaxin, 2018. Impact of low-pressure systems on winter heavy air pollution in the northwest sichuan basin. *China. Atmos. Chem. Phys.* <https://doi.org/10.5194/acp-18-13601-2018>.
- Ning, G., Yim, S.H.L., Wang, S., Duan, B., Nie, C., Yang, X., Wang, J., Shang, K., 2019. Synergistic effects of synoptic weather patterns and topography on air quality: a case of the sichuan basin of China. *Clim. Dyn.* 53, 6729–6744. <https://doi.org/10.1007/s00382-019-04954-3>.
- Olivier, J., Peters, J., Granier, C., Petron G., Müller J.F., Wallens S., 2003. Present and future surface emissions of atmospheric compounds, POET report #2, EU project EVK2-1999-00011, 2003.
- Peng, R.D., Bell, M.L., Geyh, A.S., McDermott, A., Zeger, S.L., Samet, J.M., Dominici, F., 2009. Emergency admissions for cardiovascular and respiratory diseases and the chemical composition of fine particle air pollution. *Environ. Health Perspect.* <https://doi.org/10.1289/ehp.0800185>.
- Penner, J.E., Eddleman, H., Novakov, T., 1993. Towards the development of a global inventory for black carbon emissions. *Atmos. Environ. Part A, Gen. Top.* [https://doi.org/10.1016/0960-1686\(93\)90255-W](https://doi.org/10.1016/0960-1686(93)90255-W).
- Philip, S., Martin, R.V., Van Donkelaar, A., Lo, J.W.H., Wang, Y., Chen, D., Zhang, L., Kasibhatla, P.S., Wang, S., Zhang, Q., Lu, Z., Streets, D.G., Bittman, S., Macdonald, D.J., 2014. Global chemical composition of ambient fine particulate matter for exposure assessment. *Environ. Sci. Technol.* <https://doi.org/10.1021/es502965b>.
- Qin, Y., Xie, S.D., 2012. Spatial and temporal variation of anthropogenic black carbon emissions in China for the period 1980–2009. *Atmos. Chem. Phys.* <https://doi.org/10.5194/acp-12-4825-2012>.
- Saikawa, E., Naik, V., Horowitz, L.W., Liu, J., Mauzerall, D.L., 2009. Present and potential future contributions of sulfate, black and organic carbon aerosols from China to global air quality, premature mortality and radiative forcing. *Atmos. Environ.* 43, 2814–2822. <https://doi.org/10.1016/j.atmosenv.2009.02.017>.
- Skamarock, W.C., Wang, W., Klemp, J.B., Dudhia, J., Gill, D.O., Barker, D.M., Duda, M.G., Huang, X., Powers, J.G., 2008. 2005: A description of the advanced research WRF version 3. NCAR Tech. Note. <https://doi.org/10.5065/D68S4MVH>.
- Streets, D.G., Aunan, K., 2005. The importance of China's household sector for black carbon emissions. *Geophys. Res. Lett.* <https://doi.org/10.1029/2005GL022960>.
- Streets, D.G., Bond, T.C., Carmichael, G.R., Fernandes, S.D., Fu, Q., He, D., Klimont, Z., Nelson, S.M., Tsai, N.Y., Wang, M.Q., Woo, J.-H., Yarber, K.F., 2003. An inventory of gaseous and primary aerosol emissions in Asia in the year 2000. *J. Geophys. Res. Atmos.* <https://doi.org/10.1029/2002JD003093>.
- Streets, D.G., Gupta, S., Waldhoff, S.T., Wang, M.Q., Bond, T.C., Yiyun, B., 2001. Black carbon emissions in China. *Atmos. Environ.* [https://doi.org/10.1016/S1352-2310\(01\)00179-0](https://doi.org/10.1016/S1352-2310(01)00179-0).
- Suglia, S.F., Gryparis, A., Wright, R.O., Schwartz, J., Wright, R.J., 2007. Association of black carbon with cognition among children in a prospective birth cohort study. *Am. J. Epidemiol.* 167, 280–286.
- Sun, D., Fang, J., Sun, J., 2018. Health-related benefits of air quality improvement from coal control in China: evidence from the Jing-Jin-Ji region. *Resour. Conserv. Recycl.* 129, 416–423. <https://doi.org/10.1016/j.resconrec.2016.09.021>.
- Tao, S., Ru, M.Y., Du, W., Zhu, X., Zhong, Q.R., Li, B.G., Shen, G.F., Pan, X.L., Meng, W.J., Chen, Y.L., Shen, H.Z., Lin, N., Su, S., Zhuo, S.J., Huang, T.B., Xu, Y., Yun, X., Liu, J.F., Wang, X.L., Liu, W.X., Cheng, H.F., Zhu, D.Q., 2018. Quantifying the rural residential energy transition in China from 1992 to 2012 through a representative national survey. *Nat. Energy.* <https://doi.org/10.1038/s41560-018-0158-4>.
- Wang, R., Tao, S., Wang, W., Liu, J., Shen, H., Shen, G., Wang, B., Liu, X., Li, W., Huang, Y., Zhang, Y., Lu, Y., Chen, H., Chen, Y., Wang, C., Zhu, D., Wang, X., Li, B., Liu, W., Ma, J., 2012. Black carbon emissions in China from 1949 to 2050. *Environ. Sci. Technol.* <https://doi.org/10.1021/es3003684>.
- Wang, H., Li, J., Gao, Z., Yim, S.H.L., Shen, H., Ho, H.C., Li, Z., Zeng, Z., Liu, C., Li, Y., Ning, G., Yang, Y., 2019. High-Spatial-Resolution Population Exposure to PM2.5 Pollution Based on Multi-Satellite Retrievals: A Case Study of Seasonal Variation in the Yangtze River Delta, China in 2013. *Remote Sensing* 11 (23). <https://doi.org/10.3390/rs11232724>.
- Wang, X., Liang, X.Z., Jiang, W., Tao, Z., Wang, J.X.L., Liu, H., Han, Z., Liu, S., Zhang, Y., Grell, G.A., Peckham, S.E., 2010. WRF-Chem simulation of East Asian air quality: Sensitivity to temporal and vertical emissions distributions. *Atmos. Environ.* <https://doi.org/10.1016/j.atmosenv.2009.11.011>.
- Wang, Y.X., McElroy, M.B., Jacob, D.J., Yantosca, R.M., 2004. A nested grid formulation for chemical transport over Asia: applications to CO. *J. Geophys. Res. D Atmos.* 109, 1–20. <https://doi.org/10.1029/2004JD005237>.
- WHO, 2012. *Health Effects of Black Carbon*. WHO.
- WHO, 2007. Indoor air pollution: national burden of disease estimates. *World Health Organ.* [https://doi.org/10.1043/1094-2831\(2006\)0027\[0016:IICSAO\]2.0.CO;2](https://doi.org/10.1043/1094-2831(2006)0027[0016:IICSAO]2.0.CO;2).
- Xu, X., 2017. China Population spatial Distribution Kilometer Grid Dataset. <https://doi.org/10.12078/2017121101>. Beijing.
- Yang, X., Teng, F., 2018. The air quality co-benefit of coal control strategy in China. *Resour. Conserv. Recycl.* <https://doi.org/10.1016/j.resconrec.2016.08.011>.
- Yang, Y., Zheng, Z., Yim, S.H.L., Roth, M., Gao, Z., Wang, T., Li, Q., Shi, C., Ning, G., Li, Y., 2020. PM2.5 Pollution Modulates Wintertime Urban Heat Island Intensity in the Beijing-Tianjin-Hebei Megalopolis, China. *Geophysical Research Letters* 47 (1). <https://doi.org/10.1029/2019GL084288>.
- Yim, S.H.L., Gu, Y., Shapiro, M.A., Stephens, B., 2019a. Air quality and acid deposition impacts of local emissions and transboundary air pollution in Japan and South Korea. *Atmospheric Chemistry and Physics* 19, 13309–13323. <https://doi.org/10.5194/acp-19-13309-2019>.
- Yim, S.H.L., Wang, M., Gu, Y., Yang, Y., Dong, G., Li, Q., 2019b. Effect of Urbanization on Ozone and Resultant Health Effects in the Pearl River Delta Region of China. *Journal of Geophysical Research: Atmospheres* 124 (21), 11568–11579. <https://doi.org/10.1029/2019JD030562>.
- Yu, E., Sun, J., Chen, H., Xiang, W., 2015. Evaluation of a high-resolution historical simulation over China: climatology and extremes. *Clim. Dyn.* <https://doi.org/10.1007/s00382-014-2452-6>.
- Yuan, J., Na, C., Lei, Q., Xiong, M., Guo, J., Hu, Z., 2018. Coal use for power generation in China. *Resour. Conserv. Recycl.* <https://doi.org/10.1016/j.resconrec.2016.03.021>.
- Zhang, Q., Streets, D.G., Carmichael, G.R., He, K.B., Huo, H., Kannari, A., Klimont, Z., Park, I.S., Reddy, S., Fu, J.S., Chen, D., Duan, L., Lei, Y., Wang, L.T., Yao, Z.L., 2009. Asian emissions in 2006 for the NASA INTEX-B mission. *Atmos. Chem. Phys.* <https://doi.org/10.5194/acp-9-5131-2009>.
- Zhang, Q., Wang, Y., Zhang, W., Xu, J., 2019a. Energy and resource conservation and air pollution abatement in China's iron and steel industry. *Resour. Conserv. Recycl.* 147, 67–84. <https://doi.org/10.1016/j.resconrec.2019.04.018>.
- Zhang, W., Jiang, L., Cui, Y., Xu, Y., Wang, C., Yu, J., Streets, D.G., Lin, B., 2019b. Effects of urbanization on airport CO2 emissions: a geographically weighted approach using nighttime light data in China. *Resour. Conserv. Recycl.* 150, 104454. <https://doi.org/10.1016/j.resconrec.2019.104454>.
- Zhang, W., Li, A., Xu, Y., Liu, J., 2018a. The theory-practice gap of black carbon mitigation technologies in rural China. *Atmos. Environ.* 174, 122–131. <https://doi.org/10.1016/j.atmosenv.2017.11.050>.
- Zhang, W., Lu, Z., Xu, Y., Wang, C., Gu, Y., Xu, H., Streets, D.G., 2018b. Black carbon emissions from biomass and coal in rural China. *Atmos. Environ.* 176. <https://doi.org/10.1016/j.atmosenv.2017.12.029>.
- Zhang, W., Stern, D., Liu, X., Cai, W., Wang, C., 2017. An analysis of the costs of energy saving and CO2 mitigation in rural households in China. *J. Clean. Prod.* 165, 734–745. <https://doi.org/10.1016/j.jclepro.2017.07.172>.
- Zhang, W., Wang, C., Zhang, L., Xu, Y., Cui, Y., Lu, Z., Streets, D.G., 2018c. Evaluation of the performance of distributed and centralized biomass technologies in rural China. *Renew. Energy* 125, 445–455. <https://doi.org/10.1016/j.renene.2018.02.109>.
- Zhao, Y., Zhang, J., Nielsen, C.P., 2013. The effects of recent control policies on trends in emissions of anthropogenic atmospheric pollutants and CO2 in China. *Atmos. Chem. Phys.* <https://doi.org/10.5194/acp-13-487-2013>.
- Zheng, Z., Ren, G., Wang, H., Dou, J., Gao, Z., Duan, C., Li, Y., Ngarukiyimana, J.P., Zhao, C., Cao, C., Jiang, M., Yang, Y., 2018. Relationship Between Fine-Particle Pollution and the Urban Heat Island in Beijing, China: Observational Evidence. *Boundary-Layer Meteorology* 169 (93–113)(2018). <https://doi.org/10.1007/s10546-018-0362-6>.
- Zheng, Y., Xue, T., Zhang, Q., Geng, G., Tong, D., Li, X., He, K., 2017. Air quality improvements and health benefits from China's clean air action since 2013. *Environ. Res. Lett.* <https://doi.org/10.1088/1748-9326/aa8a32>.
- Zhou, Y., Xing, X., Lang, J., Chen, D., Cheng, S., Wei, L., Wei, X., Liu, C., 2017. A comprehensive biomass burning emission inventory with high spatial and temporal resolution in China. *Atmos. Chem. Phys.* <https://doi.org/10.5194/acp-17-2839-2017>.